

# The quantitative reconstruction of temperature and precipitation in the Guanzhong Basin of the southern Loess Plateau between 6200 BP and 5600 BP

The Holocene  
2016, Vol. 26(8) 1200–1207  
© The Author(s) 2016  
Reprints and permissions:  
sagepub.co.uk/journalsPermissions.nav  
DOI: 10.1177/0959683616638417  
hol.sagepub.com  


Nan Sun,<sup>1,2,3</sup> Xiaoqiang Li,<sup>3</sup> John Dodson,<sup>4</sup> Xinying Zhou,<sup>3</sup>  
Keliang Zhao<sup>3</sup> and Qing Yang<sup>3</sup>

## Abstract

Understanding the features of the paleoclimate and paleoenvironment from key areas is crucial for predicting the climate variation of the future. In this study, fossil charcoal coupled with high-accuracy accelerator mass spectrometry (AMS) <sup>14</sup>C dating from the Guanzhong Basin is analyzed to reconstruct the paleoclimate. Here, the coexistence approach (CA) was applied, and the result showed that the mean annual temperature (MAT) was about 14.8°C, and the annual precipitation (AP) was about 831.1 mm in the Guanzhong Basin during 6200–5600 cal. a BP. Comparing the climate between the mid-Holocene and present in the Xi'an area, the MAT was about 1.1°C higher than today and the AP was about 278 mm higher than today, similar to the modern climate of the Hanzhong area in the southern Qinling Mountains.

## Keywords

fossil charcoal, Guanzhong Basin, loess plateau, mid-Holocene, paleoprecipitation, paleotemperature

Received 12 October 2015; revised manuscript accepted 13 January 2016

## Introduction

'Global Warming' has a profound impact on governments and people worldwide; however, the warming extent and its climatic–ecological effects are still uncertain. In order to understand and predict climate changes in the future, one approach is to study the features of the paleoclimate and paleoenvironment variation from key areas, identify historical analogues of predicted warming, and reconstruct the paleotemperature and paleoprecipitation from robust climatic proxies.

The early-Holocene experienced increased temperatures, and then, a warm and humid mid-Holocene was followed by a cooling trend of the late-Holocene (Marcott et al., 2013; Wang et al., 2005). The Holocene Megathermal occurred in the mid-Holocene (An et al., 2000; Renssen et al., 2009; Salonen et al., 2011; Wanner et al., 2008), when the mean global temperature was about 1–2°C higher than today and is similar to scenarios of future global warming (IPCC, 2013). The Megathermal Maximum in China occurred during 8–6.4 ka BP when the temperature was about 1.5°C higher (Fang and Hou, 2011) and the precipitation was about 50–300 mm higher than today (Fang et al., 2011), but these values are very generalized. The warming extent varies from eastern to western China (Ge et al., 2006), indicating regional differences (Steig, 1999). Therefore, it is important to obtain high-resolution climatic records from different areas, which can help us better understanding the processes and patterns of climate change (Broecker, 1997; Steig, 1999).

The Chinese Loess Plateau (CLP) is in a semi-arid and sub-humid area of middle and western China and the climate is strongly controlled by the East Asian monsoon. The ecosystems

are fragile and sensitive to climate change (Gong and Wang, 2005), and thus, this area is significant for carrying out research on response to climate changes. To date, some achievements have been made. A pollen and lake record from the western CLP indicates that the wettest period in the Holocene appears during 7.5–5.9 cal. ka BP (An et al., 2003). Fossil charcoal from the Tianshui Basin shows that the mean annual temperature (MAT) was approximately 13.2°C, and the annual precipitation (AP) was approximately 778 mm between 5.2 and 4.3 cal. ka BP (Sun and Li, 2012). Magnetic susceptibility analysis from Luochuan, which is located in the middle of the CLP, suggests that the MAT reached a maximum of  $12.2 \pm 1.4^\circ\text{C}$  and the AP peaked at  $701 \pm 74$  mm during the Holocene (Lu et al., 1994). Organic stable carbon isotopic composition data from a loess-sand sequence which

<sup>1</sup>School of Earth Science and Resources, Chang'an University, China

<sup>2</sup>Key Laboratory for the Study of Focused Magmatism and Giant Ore Deposits, MLR, China

<sup>3</sup>Key Laboratory of Vertebrate Evolution and Human Origins, Institute of Vertebrate Paleontology and Paleoanthropology, Chinese Academy of Sciences, China

<sup>4</sup>School of Earth and Environment, University of Wollongong, Australia

## Corresponding author:

Xiaoqiang Li, Key Laboratory of Vertebrate Evolution and Human Origins, Institute of Vertebrate Paleontology and Paleoanthropology, Chinese Academy of Sciences, Beijing 100044, China.  
Email: lixiaoqiang@ivpp.ac.cn

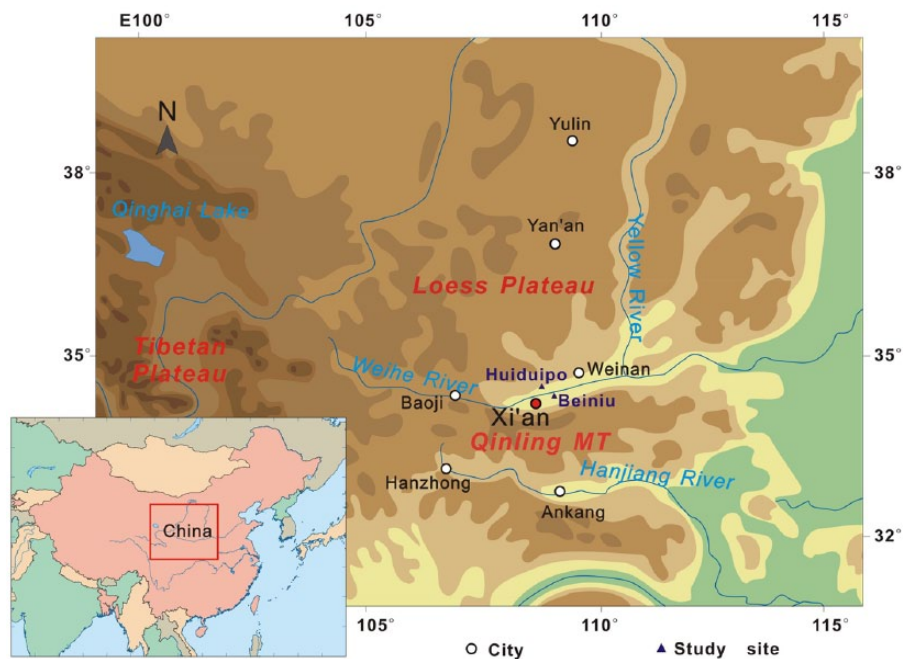


**Figure 1.** Study area.

is located to the north of the CLP indicate that the AP was 435 mm after 8 ka (Chen et al., 2015). Nevertheless, the Loess Plateau covers a large area, the climate character varies from west to east and from north to south, and paleoclimate data from each part of the CLP will make a contribution toward a more thorough understanding of the climate change mechanisms in this region. The Guanzhong Basin is located on the southern CLP, and it covers about 300 km from west to east. In the west Guanzhong Basin, plant phytolith assemblages from Baoji indicate that the MAT was 14–16°C and the AP was 700–800 mm during the Holocene (Lu et al., 1996). In the east Guanzhong Basin, the geochemical transfer functions from Weinan show that the MAT was about 12–14°C and the AP was above 700 mm during the Holocene optimum (Sun et al., 1999a). However, data on paleoclimates from the hinterland were insufficient; this study will broaden the paleoclimate database of the CLP.

Botanical records are important proxies for paleoclimate studies; for example, pollen (Huntley, 1993; Seppä and Birks, 2001; Seppä et al., 2004), plant macrofossils (Yao et al., 2011), fruits (Grein et al., 2011), and fossil charcoal (Sun and Li, 2012) have been used. Pollen sites for analysis are rare in the CLP, and it has proven difficult to quantitatively reconstruct the paleoclimate of the region based on pollen. Fortunately, Neolithic culture and early agriculture flourished in the CLP, and many relics such as fossil charcoal are well preserved in Neolithic sites. Fossil charcoal comes from the incomplete burning of wood, and the anatomical characters of the original wood are retained (McGinnes et al., 1974); this raises the possibility of much greater precision in the level of taxonomic identification, overcoming the limitation of some plant microfossils, thus improving the reliability of paleoclimate reconstruction. Therefore, fossil charcoals are ideal material for this study.

The Holocene Megathermal refers to the warmest interglacial period after the last glacial, and in this period, agriculture-based Neolithic culture developed rapidly and the Yangshao culture reached a peak in Neolithic prosperity. In order to find out the possible connections between environment and human cultures, two Yangshao culture (mid-Holocene) sites from the Guanzhong Basin around Xi'an area were selected; the fossil charcoal, with high-precision accelerator mass spectrometry (AMS)  $^{14}\text{C}$  dating, was analyzed to quantify the paleoclimate for the period.

## Study area

The Guanzhong Basin is located in the middle region of the Yellow River valley; it is bounded on the west by Baoji, the east by Tongguan, and the south by the Qinling Mountains. Because of its special geographic setting, a warm-humid climate developed in this area made it an ideal place for settlements. The Neolithic cultures include the Laoguantai, Yangshao, and the Longshan cultures, and they were well developed in the Guanzhong Basin, making the Guanzhong Basin recognition as the cradle of Chinese civilization. Xi'an is located in the hinterland of the Guanzhong Basin, with annual temperature of 13.7°C and AP of 553.3 mm, and two Yangshao culture sites including Huiduipo and Beiniu sites near Xi'an were selected for this study.

The Huiduipo site (34°34'4.1"N, 109°01'41.8"E) located in the Huiduipo village of Gaoling county, in Xi'an city (Figure 1), is a site that covers an area of 60,000 m<sup>2</sup>, and the culture layer is about 5 m thick. Relics such as red and black clay pottery are common in the site. A 300-cm-deep sediment profile with abundant fossil charcoals from the southern site was selected for this study, and three layers were divided according to the color and lithologic features of the sediment (Figure 2): above 20 cm is the modern cultivation layer, containing grass roots; between 20 and 240 cm, there is a brownish culture layer, containing abundant charcoal fragments and pottery pieces; below 240 cm is yellowish unconsolidated loess.

The Beiniu site (34°28'14.5"N, 109°01'2.6"E) is located in Beiniu village of Lintong county, in Xi'an city, and is close to the southern bank of the Weihe River (Figure 1). Extensive excavation projects have been conducted at the Beiniu site by the Shaanxi Provincial Institute of Archaeology, and its area of 200,000 m<sup>2</sup> has relics such as gray and red pottery (Sun et al., 2006). A 300-cm-deep sediment profile with abundant fossil charcoals from the eastern site was selected for this study, and eight layers were divided according to the color and lithologic features of the sediment (Figure 2): (1) 0–10 cm: modern cultivation layer, containing grass roots; (2) 10–50 cm: yellowish unconsolidated loess; (3) 50–70 cm: blackish cultural layer, containing many charcoal fragments and pottery pieces; (4) 70–100 cm: brownish cultural layer, containing a few charcoal fragments and pottery pieces; (5) 100–200 cm: blackish cultural layer; (6) 200–210 cm: brownish

cultural layer; (7) 210–280 cm: blackish cultural layer; (8) 280–300 cm: yellowish unconsolidated loess.

## Methods

Two sections with continuous and undisturbed cultural sediment in the Huiduipo and Beiniu sites were selected; the fossil charcoal and seeds within the sediment were recovered using the floatation method (Tsuyuzaki, 1994). In this study, nine AMS radiocarbon dates were measured at the Australian Nuclear Science and Technology Organization (ANSTO) based on recovered seeds, and the conventional  $^{14}\text{C}$  ages were then converted to calibrated ages using the IntCal09 dataset (Reimer et al., 2009) (Table 1). Other ages were inferred from interpolation between dated samples.

Based on a statistical analysis of fossil charcoal from temperate regions (Keepax, 1988; Smart and Hoffman, 1988; Sun and Li, 2012), a minimum of about 100 pieces of fossil charcoal from each sample is considered suitable for reliable analysis. Fossil charcoal samples were selected at random, following standard procedures: first, pressure fractured charcoal fragments were prepared with a razor blade, in order to produce fresh clean surfaces to show transverse, radial, and tangential sections (Leney and Casteel, 1975). These were examined under a stereomicroscope, categorized, and one or two samples from each type were photographed under a scanning electron microscope (SEM). Identification of the taxa was carried out using wood anatomy atlases (Cheng et al., 1985; Schweingruber, 1990; Yao, 1988; Yao et al., 2002).

The coexistence approach (CA) is a method for quantitative reconstruction of paleoclimate (Mosbrugger and Utescher, 1997), and it performs well for lowland and mid-altitude areas (Grimm and Denk, 2012), the reliability of which has been validated by previous studies (Sun and Li, 2012; Yang et al., 2007). It is based on the assumption that fossil plants have similar climatic requirements as their nearest living relative species (NLRS), and while the climatic requirements for each NLRS may be different, the overlap interval of the climatic data from different fossil plants is supposed to be the paleoclimate when the fossil plants co-existed (Mosbrugger and Utescher, 1997). Since plants in the Holocene are the result of long-term natural selection, their ecological amplitude and climatic tolerance are assumed to be the same as their living plant counterparts; thus, the CA is well suited for obtaining quantitative information about past climate.

Most published CA analyses rely on climate data for NLRS stored in the paleoflora database (PFDB). However, this database is mainly from North American and European species and is incomplete for China which is a region of megadiversity. The distribution characteristic of modern plants in China is well known, and distribution maps for more than 11,000 species at the level of counties are documented in the 'Atlas of woody plants in China' (Fang et al., 2009). This provides information on both species and environmental variables, including MAT ( $^{\circ}\text{C}$ ), annual biotemperature (ABT,  $^{\circ}\text{C}$ ), warmth index (WI,  $^{\circ}\text{C}$ ), coldness index (CI,  $^{\circ}\text{C}$ ), AP (mm), and seven other climatic variables (Fang et al., 2009; Kou, 2005). Here, two main climatic factors are calculated: MAT and AP based on the database from the atlas.

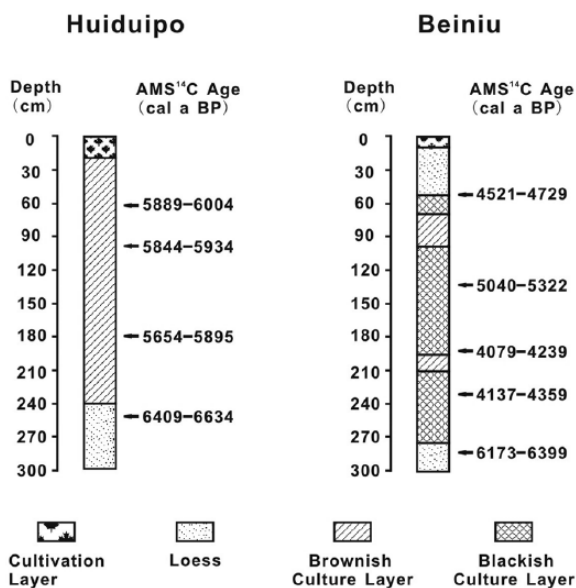


**Figure 2.** Stratigraphic sections from the Huiduipo and the Beiniu sites.

## Results

### Huiduipo site

The AMS radiocarbon dates from the Huiduipo section show that the sediment was deposited between 6500 and 5600 cal. a BP (Table 1). In order to obtain sufficient charcoal fragments for quantitative analysis, six samples were selected from the sediment between 20 and 200 cm depth that was deposited between 6300 and 5600 cal. a BP.

A total of 516 charcoal fragments from six samples were examined, and 17 different taxa were identified with one unknown species (Table 2). The abundance of *Quercus* sp. (14.92%), *Fargesia* sp. (13.37%), *Ulmus* sp. (12.02%), *Sassafras* sp. (9.88%), and *Salix* sp. (9.11%) make up about 60% of the fossil charcoal assemblages, while *Abies* sp. (7.56%), *Vitis* sp. (6.59%), and *Toxicodendron* sp. (4.84%) have lower abundance. It is worth noting that five subtropical taxa *Castanopsis* sp., *Fargesia* sp., *Sassafras* sp., *Stewartia* sp., and *Toxicodendron* sp. appear in the charcoal assemblages.

### Beiniu site

The AMS radiocarbon dates and the interpolation dates from the Beiniu section show that the sediment was deposited between 6200

**Table 1.** Accelerator mass spectrometry (AMS) radiocarbon dates from the Huiduipo (HDP) and the Beiniu (BN) sites.

Sample code	Depth (cm)	Lab code	AMS $^{14}\text{C}$ age (a BP)	Calibrated age ( $2\delta$ )	Mean age (cal. a BP)
HDP3	60	OZM470	5183 $\pm$ 39	5889–6004	5947
HDP5	100	OZM471	5121 $\pm$ 35	5844–5934	5889
HDP9	180	OZM472	5015 $\pm$ 45	5654–5895	5775
HDP13	250	OZM473	5718 $\pm$ 47	6409–6634	6522
BN1	60	OZM477	4111 $\pm$ 38	4521–4729	4625
BN5	140	OZM478	4541 $\pm$ 49	5040–5322	5181
BN8	200	OZM479	3769 $\pm$ 31	4079–4239	4159
BN10	240	OZM480	3820 $\pm$ 45	4137–4359	4248
BN13	300	OZM481	5451 $\pm$ 69	6173–6399	6286

**Table 2.** The fossil charcoal assemblages from the Huiduipo site during 6300–5600 cal. a BP.

Taxa	Absolute fragment count	Abundance ratio (%)	Ubiquity	Frequency (%)
<i>Abies</i> sp.	39	7.56	5	83.33
<i>Berchemia</i> sp.	16	3.10	3	50
<i>Castanopsis</i> sp.	13	2.52	5	83.33
<i>Clematis</i> sp.	7	1.36	4	66.67
<i>Cotoneaster</i> sp.	9	1.74	3	50
<i>Fargesia</i> sp.	69	13.37	5	83.33
<i>Prunus</i> sp.	13	2.52	3	50
<i>Quercus</i> sp.	77	14.92	6	100
<i>Rhamnus</i> sp.	6	1.16	2	33.33
<i>Salix</i> sp.	47	9.11	6	100
<i>Sassafras</i> sp.	51	9.88	6	100
<i>Stewartia</i> sp.	8	1.55	4	66.67
<i>Toxicodendron</i> sp.	25	4.84	3	50
<i>Ulmus</i> sp.	62	12.02	5	83.33
<i>Vitis</i> sp.	34	6.59	5	83.33
<i>Wikstroemia</i> sp.	19	3.68	3	50
Unknown	21	4.07	6	100
Total	516	100	6	100

**Table 3.** The fossil charcoal assemblages from the Beiniu site during 6200–5600 cal. a BP.

Taxa	Absolute fragment count	Abundance ratio (%)	Taxa	Absolute fragment count	Abundance ratio (%)
<i>Carpinus</i> sp.	10	2.03	<i>Paliurus</i> sp.	139	28.2
<i>Castanopsis</i> sp.	5	1.01	<i>Pinus</i> sp.	57	11.56
<i>Cornus</i> sp.	8	1.62	<i>Platycarya</i> sp.	28	5.68
<i>Cyclobalanopsis</i> sp.	28	5.68	<i>Quercus</i> sp.	134	27.18
<i>Fargesia</i> sp.	14	2.84	<i>Rhamnus</i> sp.	8	1.62
<i>Gleditsia</i> sp.	4	0.81	<i>Sinowilsonia henryi</i> Hemsl	19	3.85
<i>Hovenia</i> sp.	10	2.03	<i>Zelkova</i> sp.	25	5.07
<i>Melia</i> sp.	4	0.81			

and 4700 cal. a BP (Table 1). A total of 704 charcoal fragments from five samples were examined, and 15 different taxa were identified (Table 3). Almost all the taxa appeared in the earlier three samples (493 charcoal fragments) dated between 6200 and 5600 cal. a BP, while many taxa disappeared in the later two samples (211 charcoal fragments) dated between 5600 and 4700 cal. a BP; here, our study will focus on the samples between 6200 and 5600 cal. a BP.

Table 3 shows that the abundance of *Paliurus* sp. (28.2%), *Quercus* sp. (27.18%), and *Pinus* sp. (11.56%) make up about 67% of the fossil charcoal assemblages, and *Cyclobalanopsis* sp. (5.68%), *Platycarya* sp. (5.68%), and *Zelkova* sp. (5.07%) are lower in abundance. Also, five subtropical taxa including *Castanopsis* sp., *Cyclobalanopsis* sp., *Fargesia* sp., *Melia* sp., and *Platycarya* sp. appear in the charcoal assemblages.

The Huiduipo and Beiniu sites are located in Xi'an – a hinterland region of the Guanzhong Basin, and they are in close proximity (Figure 1); as mentioned above, the AMS <sup>14</sup>C dating of the samples from the two sites used here is 6300–5600 and 6200–5600 cal. a BP, respectively. For this reason, the climate and environment of the two sites are assumed to be similar during 6200–5600 cal. a BP, and the plant taxa found in the two sites is due to environmental preferences related to climate; therefore, the plant taxa from both the Huiduipo and Beiniu site will reflect the climate in the Guanzhong Basin between 6200 and 5600 cal. a BP.

After combining the fossil charcoal taxa from the two sites, we observe a total of 27 taxa (duplicate records were deleted) appeared in the study area during the mid-Holocene, and the climatic factors were obtained from the CA analysis based on these fossil charcoal taxa. The CA results show that the MAT was

9–15.8°C, and the AP was 760–1478 mm in the Guanzhong Basin during 6200–5600 cal. a BP (Figure 3).

## Discussion

### Evaluation and validation on the quantitative reconstructions

The Guanzhong Basin is located in the transition area between the Qinling Mountains and the CLP (Figure 1). The Qinling Mountains lie across central China and is an important dividing line of vegetation and climate, with subtropical climate in the south and warm temperate climate in the north; accordingly, subtropical evergreen broadleaf forest is developed on the south and temperate deciduous forest on the north slopes. The modern climate of the CLP is governed by the East Asian monsoon system, and it shows a regular pattern from north to south; the climate changes gradually from cold and dry to warm and wet, and this brings a corresponding change in the vegetation type from north to south. In order to find the relationship between vegetation and climate in the study area, and verify the validity of the CA in quantitative reconstruction of the paleoclimate, CA is applied to the modern vegetation types of different climatic zones to obtain the estimated value of climatic factors, which will be effectively compared with the actual climatic factors.

According to the climate character of the CLP, a belt around the Guanzhong Basin from the desert/loess transition zone to the south slopes of the Qinling Mountains was selected; five places including Shenmu (which is located in Yulin), Yan'an, Xi'an, Hanzhong, and Ankang (Figure 1) were chosen to carry out a vegetation–climate relationship study. In this paper, most of the charcoal fragments were identified to genus and a few to species level; hence, different

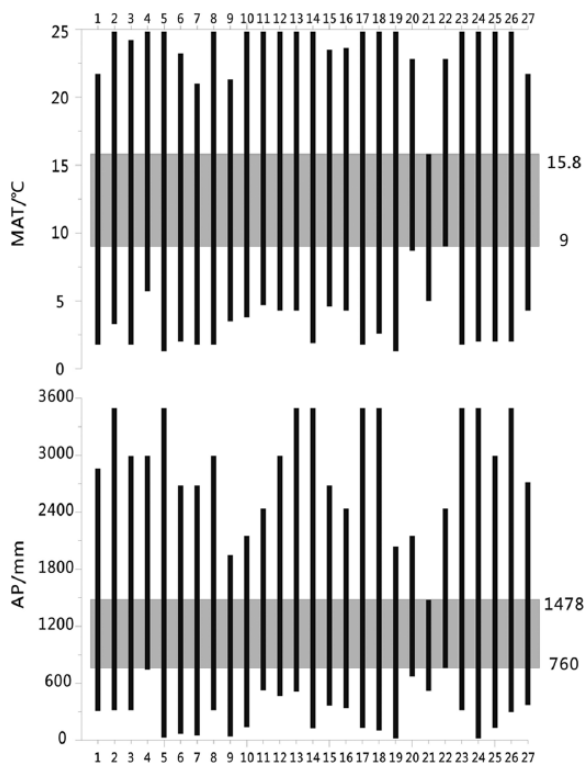


**Figure 3.** Coexistence intervals for Xi'an during 6200–5600 cal. a BP. 1. *Abies* sp.; 2. *Berchemia* sp.; 3. *Carpinus* sp.; 4. *Castanopsis* sp.; 5. *Clematis* sp.; 6. *Cornus* sp.; 7. *Cotoneaster* sp.; 8. *Cyclobalanopsis* sp.; 9. *Fargesia* sp.; 10. *Gleditsia* sp.; 11. *Hovenia* sp.; 12. *Melia* sp.; 13. *Paliurus* sp.; 14. *Pinus* sp.; 15. *Platycarya* sp.; 16. *Prunus* sp.; 17. *Quercus* sp.; 18. *Rhamnus* sp.; 19. *Salix* sp.; 20. *Sassafras* sp.; 21. *Sinowilsonia henryi* Hemsl.; 22. *Stewartia* sp.; 23. *Toxicodendron* sp.; 24. *Ulmus* sp.; 25. *Vitis* sp.; 26. *Wikstroemia* sp.; 27. *Zelkova* sp.

genera of the local modern woody plants from the five places were selected according to local chronicles and the Flora of China (Ankang Local Chronicles Compilation Committee, 1989; Du, 2009; Flora of China Editorial Committee of Chinese Academy of Sciences, 2004; Hanzhong Local Chronicles Compilation Committee, 1994; Shenmu County Chronicles Compilation Committee, 1990; Xi'an Local Chronicles Compilation Committee, 1996; Yan'an Local Chronicles Compilation Committee, 1994), related modern climatic factors come from the Surface Meteorological Data of China (1971–2000, Table 4).

Based on the climate information of each plant from the 'Atlas of Woody Plants in China' (Fang et al., 2009), CA analysis was applied to the modern woody plants in the five places to obtain the estimated climatic factors, including the lowest and the highest estimated value of MAT (MATmin, MATmax) and AP (APmin, APmax), and then the correlation between estimates and actual value (MAT, AP) was analyzed (using Statistical Package for the Social Science (SPSS)). Table 5 shows that the Pearson correlation coefficient is 0.986, which indicates that the correlation between the independent variables (MATmax, MATmin) and the dependent variable (MAT) is high;  $R^2$  is 0.973, thus about 97% of the variation in the dependent variable can be explained by the variation in the independent variable and thus estimated temperature is close to the actual temperature; the significance level of the  $F$  test is 0.027 (Table 6); therefore, the regression equation established here is strong. Based on the regression coefficients (Table 7), the equation showing the relationship is as follows:

$$\text{MAT} = 0.057 + 1.13\text{MATmin} + 0.287\text{MATmax} \quad (1)$$

Table 8 shows that the Pearson correlation coefficient is 0.992, which indicates that the correlation between the independent variables (APmax, APmin) and the dependent variable (AP) is high;  $R^2$  is 0.984,

indicating that about 98% of the variation in the dependent variable can be explained by the variation in the independent variable, thus estimated precipitation is close to the actual precipitation; the significance level of the  $F$  test is 0.016 (Table 9), hence the regression equation established here is also strong. Based on the regression coefficients (Table 10), the equation is established as follows:

$$\text{AP} = 123.217 + 0.737\text{APmin} + 0.1\text{APmax} \quad (2)$$

Climate plays an important role in controlling vegetation distribution, and climate change will therefore cause vegetation shifts southwards or northwards (Ni et al., 2010; Prentice et al., 2000; Sun et al., 1999b; Yu et al., 1998, 2000); also, the shift can occur in the belt from the desert/loess transition zone in the north to the south slope of the Qinling Mountains. Thus, natural vegetation types around Xi'an can shift in sympathy with northern (e.g. Yan'an, Shenmu) or southern neighbors (e.g. Hanzhong, Ankang) depending on the climate changes. Since the regression equations applicable to each place in this belt today, we assume that it is applicable for Xi'an during the mid-Holocene.

The estimated climatic factors of the Xi'an area obtained from the CA analysis are as follows: MATmin = 9°C, MATmax = 15.8°C; APmin = 760 mm, APmax = 1478 mm; in order to find the most probable value of the MAT and AP in the study area, the estimated values are substituted into Eqs (1) and (2), respectively, and the result shows that the MAT was about 14.8°C and the AP was about 831.1 mm in Xi'an area between 6200 and 5600 cal. a BP. Thus, in the mid-Holocene, the MAT was about 1.1°C higher than today and the AP was about 278 mm higher than today for Xi'an, these are similar to the modern climate of the Hanzhong area in southern Shaanxi in the southern Qinling Mountains (Figure 1; Table 11).

Paleoclimate reconstructions from west (Baoji), hinterland (Xi'an), and east (Weinan) of the Guanzhong Basin during the Holocene now exist. After comparing the paleo and modern climate data (Table 12), we see that the temperature was about 1–2°C higher, and precipitation was about 200–300 mm higher than today across the Guanzhong Basin.

### Implications of paleoclimatic reconstructions

Many studies show that water vapor in the atmosphere closely follows temperature in agreement with the Clausius–Clapeyron relationship. An increase in temperature by 1°C in the lower troposphere implies an increase in the vertical profile of water vapor by 6–7% (Bengtsson, 2010), this will cause an increase in precipitation in the East China Sea and South China Sea (Deng et al., 2014). And it is predicted that the precipitation will also increase where the rise in sea surface temperature exceeds the mean surface warming in the tropics (Huang et al., 2013; Vecchi and Soden, 2007; Xie et al., 2010).

The results of Climate simulations demonstrate that global warming would enhance the thermal depression over the Asian continent in summer, which will further enhance the East Asian Summer Monsoon (EASM). Simultaneously, the increase in water vapor in the tropics area will provide sufficient water vapor resource for the East Asia; thus, future warming will likely cause an increase in precipitation in the EASM region (Sun and Ding, 2010). Precipitation in the CLP is mainly controlled by the water vapor transported by the EASM (An et al., 2000; Chen et al., 1991; Tan et al., 2014); for this reason, increasing temperature may have a positive impact on the precipitation in the CLP.

### Human activity and its response to climate change in mid-Holocene

In the long history, food is essential for human survival and development, and the origin of agriculture guarantees that people could

**Table 4.** The modern climate and estimated climate from CA.

Locality	Actual climatic factors		Estimated climatic factors			
	MAT (°C)	AP (mm)	MATmin (°C)	MATmax (°C)	APmin (mm)	APmax (mm)
Shenmu	8	437.9	4.3	13.2	337	856
Yan'an	9.93	511.2	4.8	13.2	372	856
Xi'an	13.7	553.3	8.2	14.9	483	856
Hanzhong	14.4	852.6	8.2	16.7	760	1478
Ankang	15.6	814.2	9.8	16.7	760	1522

MAT: mean annual temperature; CA: coexistence approach; AP: annual precipitation.

**Table 5.** Model summary<sup>a</sup> (for MAT).

Model	R	R <sup>2</sup>	Adjusted R <sup>2</sup>	Standard error of the estimate
I	0.986 <sup>b</sup>	0.973	0.945	0.75109

MAT: mean annual temperature.

<sup>a</sup>Dependent variable: MAT.

<sup>b</sup>Predictors: constant, MATmax, MATmin.

**Table 6.** ANOVA<sup>a</sup> (for MAT).

Model		Sum of squares	df	Mean square	F	Sig.
I	Regression	40.235	2	20.118	35.661	0.027 <sup>b</sup>
	Residual	1.128	2	0.564		
	Total	41.364	4			

ANOVA: analysis of variance; MAT: mean annual temperature.

<sup>a</sup>Dependent variable: MAT.

<sup>b</sup>Predictors: constant, MATmax, and MATmin.

**Table 7.** Coefficients<sup>a</sup> (for MAT).

Model		Unstandardized coefficients		Standardized coefficients	t	Sig.
		B	Standard error	Bate (β)		
I	Constant	0.057	5.948		0.010	0.993
	MATmin	1.130	0.421	0.839	2.682	0.115
	MATmax	0.287	0.575	0.156	0.499	0.667

MAT: mean annual temperature.

<sup>a</sup>Dependent variable: MAT.

**Table 8.** Model summary<sup>a</sup> (for AP).

Model	R	R <sup>2</sup>	Adjusted R <sup>2</sup>	Standard error of the estimate
I	0.992 <sup>b</sup>	0.984	0.968	33.27815

AP: annual precipitation.

<sup>a</sup>Dependent variable: AP.

<sup>b</sup>Predictors: constant, APmax, and APmin.

**Table 9.** ANOVA<sup>a</sup> (for AP).

Model		Sum of squares	df	Mean square	F	Sig.
I	Regression	138090.541	2	69045.271	62.347	0.016 <sup>b</sup>
	Residual	2214.871	2	1107.435		
	Total	140305.412	4			

ANOVA: analysis of variance; AP: annual precipitation.

<sup>a</sup>Dependent variable: AP.

<sup>b</sup>Predictors: constant, APmax, and APmin.

have a reliable supply of it. China is the origin and development center of rain-fed millet (Lu et al., 2009; Zhao, 1998) and

cultivated rice (Crawford, 2006; Yan, 1997). Rain-fed agriculture was distributed mainly in the Yellow River valley in North China (Barton et al., 2009), and the common millet first appeared around 10 ka BP and the foxtail millet came after that (Lu et al., 2009). The origin and domestication of the millet are considered to be closely related to the typical climate (rain hot during the same period) of the East Asian monsoon area. Because of the sufficient precipitation, the millet cultivation spread rapidly to all over the CLP by 7 ka BP, and subsequent development of millet agriculture resulted in the flourishing of the Yangshao Culture (Huang et al., 2004). The higher temperature and precipitation during the Yangshao period (this paper) created a warm and wet environment which was able to meet the needs of rice cultivation, and this is supposed to be one of the reasons that rice spread into the Guanzhong Basin during this period (Zhang et al., 2010). The emergence of both millet and rice in the Guanzhong Basin indicates that the human farming activity changed from millet cultivation to mixed millet–rice cultivation (dominantly cultivated millets and locally cultivated rice), and this would significantly change the proportion of food production in the Neolithic subsistence economy, thus establish a very strong basis for the formation of the social civilization.

**Table 10.** Coefficients<sup>a</sup> (for AP).

Model		Unstandardized coefficients		Standardized coefficients	t	Sig.
		B	Standard error	Bate ( $\beta$ )		
I	Constant	123.217	60.191		2.047	0.177
	APmin	0.737	0.305	0.809	2.417	0.137
	APmax	0.100	0.178	0.188	0.562	0.631

AP: annual precipitation.

<sup>a</sup>Dependent variable: AP.

**Table 11.** The comparison of the climatic factors between Xi'an and Hanzhong.

Locality	Period (cal. a BP)	MAT (°C)	MAP (mm)
Xi'an	6200–5600	14.8	831.1
Xi'an	Present	13.7	553.3
Hanzhong	Present	14.4	852.6

MAT: mean annual temperature; MAP: mean annual precipitation.

**Table 12.** The comparison of the paleoclimate during the Holocene and modern climate in the Guanzhong Basin.

Locality	MAT (°C)		MAP (mm)		References
	Holocene	Modern	Holocene	Modern	
Xi'an	14.8	13.7	831.1	553.3	This paper
Baoji	14–16	13.1	700–800	656.3	Lu et al. (1996)
Weinan	12–14	13.4	>700	583.6	Sun et al. (1999a)

MAT: mean annual temperature; MAP: mean annual precipitation.

## Conclusion

The quantitative reconstruction of the paleoclimate in the hinterland of the Guanzhong Basin suggests that the MAT was 14.8°C, and the AP was about 831.1 mm. Higher temperature corresponds with the higher precipitation, which would favor the growth of subtropical plants taxa and then may cause vegetation shift northward. In this case, a warmer–wetter environment will develop in the south of the CLP if the temperature rises about 1–2°C in the future.

## Funding

This work was supported by the Chinese National Natural Science Foundation (grant nos 41202131 and 41372175); Natural Science Basic Research Plan in Shaanxi Province of China (grant no. 2016JQ4026) the Special Fund for Basic Scientific Research of Central Colleges, Chang'an University, China (grant nos 2014G1271059 and 2014G3272013); and Strategic Priority Research Program of the Chinese Academy of Sciences (grant no. XDB03020303).

## References

- An CB, Feng ZD, Tang LY et al. (2003) Environmental changes and cultural transition at 4 cal. ka BP in Central Gansu. *Acta Geographica Sinica* 58(5): 743–748.
- An ZS, Porter SC, Kutzbach JE et al. (2000) Asynchronous Holocene optimum of the East Asian monsoon. *Quaternary Science Reviews* 19(8): 743–762.
- Ankang Local Chronicles Compilation Committee (1989) *Annals of Ankang County*. Xi'an: Shaanxi People's Education Press.
- Barton L, Newsome SD, Chen FH et al. (2009) Agricultural origins and the isotopic identity of domestication in northern China. *Proceedings of the National Academy of Sciences of the United States of America* 106: 5523–5528.

- Bengtsson L (2010) The global atmospheric water cycle. *Environmental Research Letters* 5: 275–295.
- Broecker WS (1997) Future directions of paleoclimate research. *Quaternary Science Reviews* 16: 821–825.
- Chen LX, Zhu QG, Luo HB et al. (1991) *East Asian Monsoon*. Beijing: China Meteorological Press.
- Chen YY, Lu HY, Yi SW et al. (2015) A preliminary quantitative reconstruction of precipitation in southern Mu Us sandy land at margin of Asian monsoon-dominated region during late Quaternary. *Journal of Geographical Sciences* 25(3): 301–310.
- Cheng JQ, Yang JJ and Liu P (1985) *Chinese Timber Chorography*. Beijing: China Forestry Publishing House.
- Crawford GW (2006) East Asian plant domestication. In: Stark MT (ed.) *Archaeology of Asia*. Malden, MA: Blackwell Publishing, pp. 77–95.
- Deng YY, Gao T, Gao HW et al. (2014) Regional precipitation variability in East Asia related to climate and environmental factors during 1979–2012. *Scientific Reports* 4: 5693. DOI: 10.1038/srep05693.
- Du JH (2009) Study on gardening tree species in Yan'an. *Journal of Yanan University* 28(1): 76–80.
- Fang JY, Wang ZH and Tang ZY (2009) *Atlas of Woody Plants in China*. Beijing: Higher Education Press.
- Fang XQ and Hou GL (2011) Synthetically reconstructed Holocene temperature change in China. *Scientia Geographica Sinica* 31(4): 385–393.
- Fang XQ, Liu CH and Hou GL (2011) Reconstruction of precipitation pattern of China in the Holocene Megathermal. *Scientia Geographica Sinica* 31(11): 1287–1292.
- Flora of China Editorial Committee of Chinese Academy of Sciences (2004) *Flora Reipublicae Popularis Sinicae*. Beijing: Science Press.
- Ge QS, Wang SB and Zheng JY (2006) Reconstruction of temperature series in China for the last 5000 years. *Progress in Natural Science* 16(6): 689–696.
- Gong JF and Wang YR (2005) Response of climate in Loess Plateau in China to global change. *Agricultural Research in The Arid Areas* 23(6): 6–11.
- Grein M, Utescher T, Wilde V et al. (2011) Reconstruction of the middle Eocene climate of Messel using palaeobotanical data. *Neues Jahrbuch für Geologie und Paläontologie, Abhandlungen* 260: 305–318.
- Grimm GW and Denk T (2012) Reliability and resolution of the coexistence approach – A revalidation using modern-day data. *Review of Palaeobotany and Palynology* 172: 33–47.
- Hanzhong Local Chronicles Compilation Committee (1994) *Annals of Hanzhong*. Beijing: Central Party School Press.
- Huang CH, Pang JL, Zhou QY et al. (2004) Holocene pedogenic change and the emergence and decline of rain-fed cereal agriculture on the Chinese Loess Plateau. *Quaternary Science Reviews* 23(23–24): 2525–2535.
- Huang P, Xie SP, Hu KM et al. (2013) Patterns of the seasonal response of tropical rainfall to global warming. *Nature Geosciences* 6: 357–361.
- Huntley B (1993) The use of climate response surfaces to reconstruct paleoclimate from Quaternary pollen and plant

- macrofossil data. *Philosophical Transactions of the Royal Society of London, Series B, Biological Sciences* 341: 215–223.
- IPCC (2013) *Climate Change 2013: The Physical Sciences Basis*. Summary for Policy makers, Contribution of Working Group I to the Fourth Assessment Report of the Intergovernmental Panel on Climate Change, September.
- Keapax CA (1988) *Charcoal analysis with particular reference to archaeological sites in Britain*. PhD Thesis, University of London.
- Kou XY (2005) *Studies on quantitative reconstruction of Cenozoic climates in China by palynological data*. PhD Dissertation, Institute of Botany, The Chinese Academy of Sciences.
- Leney L and Casteel RW (1975) Simplified procedure for examining charcoal specimens for identification. *Journal of Archaeological Science* 2: 153–159.
- Lu HY, Han JM, Wu NQ et al. (1994) Magnetic susceptibility of Chinese modern soil and its paleoclimatic significance in China. *Science in China: Series B* 24(12): 1290–1297.
- Lu HY, Wu NQ, Liu TS et al. (1996) Seasonal climatic variation recorded by phytolith assemblages from the Baoji loess sequence in central China over the last 150 000. *Science in China: Series D* 39(6): 629–639.
- Lu HY, Zhang JP, Liu KB et al. (2009) Earliest domestication of common millet (*Panicum miliaceum*) in East Asia extended to 10,000 years ago. *Proceedings of the National Academy of Sciences of the United States of America* 106: 7367–7372.
- McGinnes EA, Szopa PS and Phelps JE (1974) Use of scanning electron microscopy in studies of wood charcoal formation. *Scanning Electron Microscopy* 1974: 469–476.
- Marcott SA, Shakun JD, Clark PU et al. (2013) A reconstruction of regional and global temperature for the past 11,300 years. *Science* 339: 1198–1201.
- Mosbrugger V and Utescher T (1997) The coexistence approach – A method for quantitative reconstructions of Tertiary terrestrial palaeoclimate data using plant fossils. *Palaeogeography, Palaeoclimatology, Palaeoecology* 134: 61–86.
- Ni J, Yu G, Harrison SP et al. (2010) Palaeovegetation in China during the late Quaternary: Biome reconstructions based on a global scheme of plant functional types. *Palaeogeography, Palaeoclimatology, Palaeoecology* 289: 44–61.
- Prentice IC, Jolly D and BIOME 6000 Members (2000) Mid-Holocene and glacial maximum vegetation geography of the northern Continents and Africa. *Journal of Biogeography* 27: 507–519.
- Reimer PJ, Baillie MGL, Bard E et al. (2009) IntCal09 and Marine09 radiocarbon age calibration curves, 0–50,000 years cal BP. *Radiocarbon* 31: 1111–1150.
- Renssen H, Seppä H, Heiri O et al. (2009) The spatial and temporal complexity of the Holocene thermal maximum. *Nature Geoscience* 2: 411–414.
- Salonen JS, Seppä H, Väliranta M et al. (2011) The Holocene thermal maximum and late-Holocene cooling in the tundra of NE European Russia. *Quaternary Research* 75: 501–511.
- Schweingruber FH (1990) *Anatomy of European Woods*. Stuttgart: Verlag Paul Haupt, Stuttgart Publishers.
- Seppä H and Birks HJB (2001) July mean temperature and annual precipitation trends during the Holocene in the Fennoscandian tree-line area: Pollen-based climate reconstructions. *The Holocene* 11: 527–539.
- Seppä H, Birks HJB, Odland A et al. (2004) A modern pollen-climate calibration set from northern Europe: Developing and testing a tool for palaeoclimatological reconstructions. *Journal of Biogeography* 31: 251–267.
- Shenmu County Chronicles Compilation Committee (1990) *Annals of Shenmu County*. Beijing: The Economic Daily Press.
- Smart TL and Hoffman ES (1988) Environmental interpretation of archaeological charcoal. In: Hastorf CA and Popper VS (eds) *Current Paleoethnobotany*. Chicago, IL and London: University of Chicago Press, pp. 165–205.
- Steig EJ (1999) Mid-Holocene climate change. *Science* 286: 1485–1487.
- Sun JM, Diao GY, Wen QZ et al. (1999a) A preliminary study on quantitative estimate of Palaeoclimate by using geochemical transfer function in the Loess Plateau. *Geochim* 28(3): 265–272.
- Sun N and Li XQ (2012) The quantitative reconstruction of the palaeoclimate between 5200 and 4300 cal. yr BP in the Tianshui Basin, NW China. *Climate of the Past* 8: 625–636.
- Sun TS, Gao MT, Du YW et al. (2006) A brief report of excavation of the Beiniu site at Lingkou town in Lintong, Shaanxi. *Archaeology and Cultural Relics* 3: 15–28.
- Sun X, Song CQ, Chen XD et al. (1999b) ‘China Quaternary Pollen Database’ (CPD) and ‘BIOME 6000’ project. *Advance in Earth Sciences* 14: 407–411.
- Sun Y and Ding YH (2010) A projection of future changes in summer precipitation and monsoon in East Asia. *Science in China: Series D* 53(2): 284–300.
- Tan LC, An ZS, Huh C-A et al. (2014) Cyclic precipitation variation on the western Loess Plateau of China during the past four centuries. *Scientific Reports* 4: 6381. DOI: 10.1038/srep06381.
- Tsuyuzaki S (1994) Rapid seed extraction from soils by a flotation method. *Weed Research* 34: 433–436.
- Vecchi GA and Soden BJ (2007) Effect of remote sea surface temperature change on tropical cyclone potential intensity. *Nature* 450: 1066–1070.
- Wang YJ, Cheng H, Edwards RL et al. (2005) The Holocene Asian monsoon: Links to solar changes and North Atlantic climate. *Science* 308(5723): 854–857.
- Wanner H, Beer J, Bütikofer J et al. (2008) Mid- to late-Holocene climate change: An overview. *Quaternary Science Reviews* 27: 1791–1828.
- Xi’an Local Chronicles Compilation Committee (1996) *Annals of Xi’an, Vol. 1*. Xi’an: Xi’an Publishing House.
- Xie SP, Deser C, Vecchi GA et al. (2010) Global warming pattern formation: Sea surface temperature and rainfall. *Journal of Climate* 23: 966–986.
- Yan WM (1997) The new progress on the rice origin in China. *Archaeology* 9: 71–76.
- Yan’an Local Chronicles Compilation Committee (1994) *Annals of Yan’an, Xi’an: Shaanxi People’s Publishing House*.
- Yang J, Wang YF, Spicer RA et al. (2007) Climatic reconstruction at the Miocene Shan wang Basin, China, using leaf margin analysis, CLAMP, coexistence approach, and over lapping distribution analysis. *American Journal of Botany* 94(4): 599–608.
- Yao XS (1988) *Structure of Main Chinese Woods*. Beijing: China Forestry Publishing House.
- Yao XS, Yi TM, Ma NX et al. (2002) *Bamboo Culm Anatomy of China*. Beijing: Science Press.
- Yao YF, Bruch AA, Mosbrugger V et al. (2011) Quantitative reconstruction of Miocene climate patterns and evolution in Southern China based on plant fossils. *Palaeogeography, Palaeoclimatology, Palaeoecology* 304: 291–307.
- Yu G, Chen X, Ni J et al. (2000) Palaeovegetation of China: A pollen data-based synthesis for the mid-Holocene and last glacial maximum. *Journal of Biogeography* 27: 635–664.
- Yu G, Prentice IC, Harrison SP et al. (1998) Pollen-based biome reconstruction for China at 0 and 6000 years. *Journal of Biogeography* 25: 1055–1069.
- Zhang JP, Lu HY, Wu NQ et al. (2010) Phytolith evidence for rice cultivation and spread in Mid-Late Neolithic archaeological sites in central North China. *Boreas* 39: 592–602.
- Zhao ZJ (1998) The Middle Yangtze region in China is one place where rice was domesticated: Phytolith evidence from the Diaotonghuan Cave, northern Jiangxi. *Antiquity* 72: 885–897.